

Reprinted from

JAPANESE JOURNAL OF
**APPLIED
PHYSICS**

REVIEW PAPER

Minute Mechanical-Excitation Wave-Front Propagation in Human Myocardial Tissue

Hiroshi Kanai and Motonao Tanaka

Jpn. J. Appl. Phys. **50** (2011) 07HA01

Minute Mechanical-Excitation Wave-Front Propagation in Human Myocardial Tissue

Hiroshi Kanai* and Motonao Tanaka¹

Graduate Schools of Biomedical Engineering and Engineering, Tohoku University, Sendai 980-8579, Japan

¹ Cardiovascular Center, Tohoku Welfare Pension Hospital, Sendai 983-0005, Japan

Received January 18, 2011; accepted March 9, 2011; published online July 20, 2011

Complexity of the cardiac contraction sequence is still not fully understood because the dynamic *mechanical excitation* process, which directly correlates with contraction, cannot be accurately measured based on the electro-magnetic phenomena. By developing a noninvasive novel imaging modality with high temporal and spatial resolutions, the present study shows that the propagation of the mechanical wave-front occurs at the beginning of cardiac contraction sequence for the first time (about 60 ms prior to the ordinarily accepted onset time of the contraction). From the apical side of the interventricular septum, a minute velocity component with an amplitude of several tenth micrometers is generated and it propagates from the apex to the base of the posterior wall, and then from the base to the apex of the septum, with a propagation speed of 3–9 m/s. This dynamic measurement modality is also applicable to various tissues in biology. © 2011 The Japan Society of Applied Physics

1. Introduction

Unlike the case of skeletal muscle, the direction of myocardial contraction does not coincide with the direction of work necessary to eject the intraventricular blood, contributing to great complexity of the wall deformation sequence of cardiac contraction. Electrocardiography is an invaluable clinical tool for the diagnosis of cardiac failure. Electrocardiographic measurement¹⁾ has realized noninvasive imaging of the spatial distribution of action potentials, and magnetocardiography²⁾ conducted inside a shielded room enables similar imaging. By these electro-magnetic phenomena-based methods, however, *mechanical properties* of myocardial velocity and contraction are not been directly measured. Other cardiac imaging tools, namely, computed tomography (CT),³⁾ magnetic resonance imaging (MRI),^{4,5)} single photon emission computed tomography (SPECT),⁶⁾ and conventional echocardiography,^{7,8)} enable visualization of two-dimensional (2D) or three-dimensional (3D) images, motion, torsional deformation, asynchronous wall motion during acute myocardial ischemia,⁹⁾ and the left ventricular inflow.¹⁰⁾ The time of peak contraction of the heart wall has been reported using 3D MRI tagging.¹¹⁾ With MRI tagging, the onset time of the contraction has been reported.^{12,13)} However, their visualization is restricted to static configurations or *large* and *slow* motion due to contraction. Using the Doppler effect of the ultrasound, the velocity or displacement are measured,^{14,15)} but an accurate waveform for which the frequency analysis is applicable is not obtained, and measurement of minute, rapid velocity waveforms at the beginning of the contraction in the heart wall has not been attempted.

We have previously found that the rapid response of the excised heart muscle of a rat to electrical stimulations is minute (displacement of 30 μm and velocity of 0.5 mm/s)¹⁶⁾ and that *velocity measurement* is superior to *displacement measurement* since the displacement is the accumulation of velocity, that is, low-pass filtering.¹⁷⁾ To realize *noninvasive* detection of such minute mechanical responses to the propagation of the action potential in the human heart, we developed a novel ultrasound-based noninvasive method¹⁸⁾ and we successfully measured such response as a velocity waveform for human subjects for the first time.¹⁹⁾ In the present study, the regional change in length or wall thickness was simultaneously measured with high temporal resolution

to confirm whether the detected velocity component corresponds to the myocardial contraction or extension.

2. Materials and Methods

In the present study, the minute propagation of the contraction/relaxation was visualized for the first time in the human as follows: The ultrasonic beams transmitted by the ultrasound probe attached to the chest wall scan the 2D plane of the heart, and the RF reflective wave for each ultrasound transmission is acquired by the same probe as in conventional echocardiography. In this novel method, however, the phase shift between the succeedingly acquired RF signals in the same direction is determined accurately at each point in the heart wall along the ultrasonic beam, and the position of each point is tracked. Thus, the minute motion at each point is measured as a velocity waveform so that the Fourier transform is applicable.^{17,20)} The six periods (atriosystolic phase, isovolumetric contraction period, ejection period, isovolumetric relaxation phase, period of rapid filling, and period of slow filling) during one cardiac cycle were characterized by the measured waveforms.²¹⁾ Moreover, by restricting the number of directions of transmission to maintain a high frame rate (500 Hz), the velocity waveforms are simultaneously obtained at about 3,000 points set in the heart wall on the 2D plane.²²⁾ Spatial distribution of the heart wall vibrations generated by remote perturbation of the inner pressure was also noninvasively measured by the method.²³⁾ By applying frequency analysis to each velocity waveform,¹⁷⁾ the phase of its 40-Hz component is detected and its instantaneous 2D distribution is reconstructed at every 2 ms, precisely revealing the minute-wave propagation in the heart wall²²⁾ by neglecting the differences in the amplitude components. The achieved lower limit in the velocity measurement has been validated as being 0.1 mm/s,²⁰⁾ which corresponds to 0.2 μm in displacement during 2 ms. Since the wavelength is about 410 μm for the typical frequency (3.75 MHz), 0.2 μm corresponds to about 1/2000 of the wavelength. Such a minute velocity component superimposed on the large motion due to heartbeat cannot be noninvasively measured by any other known method. At the same time, the regional change in length of thickness is accurately obtained from the spatial difference between the velocity waveform at the adjacent points (820 μm apart) with 0.5- μm accuracy.²⁴⁾ The propagation of the contraction in the heart wall was detected just at the apical side of the interventricular septum.²⁵⁾

*E-mail address: kanai@ecei.tohoku.ac.jp

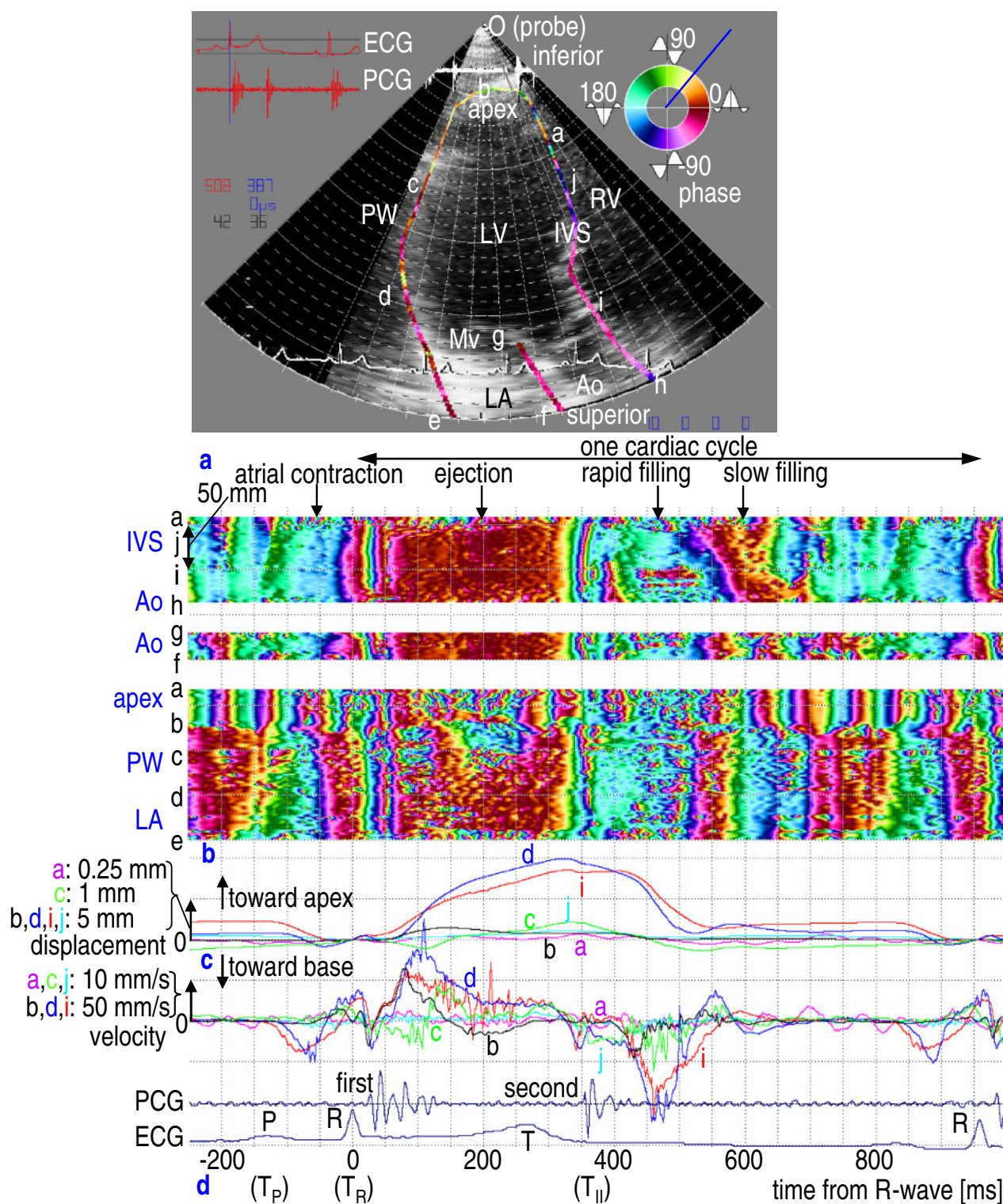


Fig. 1. (Color online) Time sequence of velocity and displacement in the unfolded left ventricular wall based on the apical view. (a) Cross-sectional image from apical view of the LV of a healthy young subject. The two colored lines passing through the walls show the phase of the 40-Hz component of the velocity wave at each point at T_R . Red and light blue correspond to the upward and downward movements, respectively. (b) Temporal changes in the phase of 40-Hz component of the velocity wave for one cardiac cycle along the two lines in (a). Vertical axis corresponds to the line in (a). (c) Displacement waveform at points a–j in (a). (d) Velocity waveform at points a–j with electrocardiogram (ECG) and phonocardiogram (PCG). (Ao = aortic valve; LA = left atrium; Mv = mitral valve; RV = right ventricle; PW = posterior wall.)

3. *In vivo* Experimental Results

By applying this novel method to the longitudinal-sectional plane of a healthy human heart as shown in Fig. 1(a), the velocity signal was measured as a waveform at each point on the plane. The velocity waveforms measured at six points

(a–j) in Fig. 1(a) and their integration, the displacement waveform, are shown in Figs. 1(d) and 1(c), respectively, for one cardiac cycle. The left ventricular (LV) contraction during the ejection period is roughly shown in the upward displacement (toward the apex) of Fig. 1(c). In the velocity waveform of Fig. 1(d), from the time of the P-wave, T_P , of the

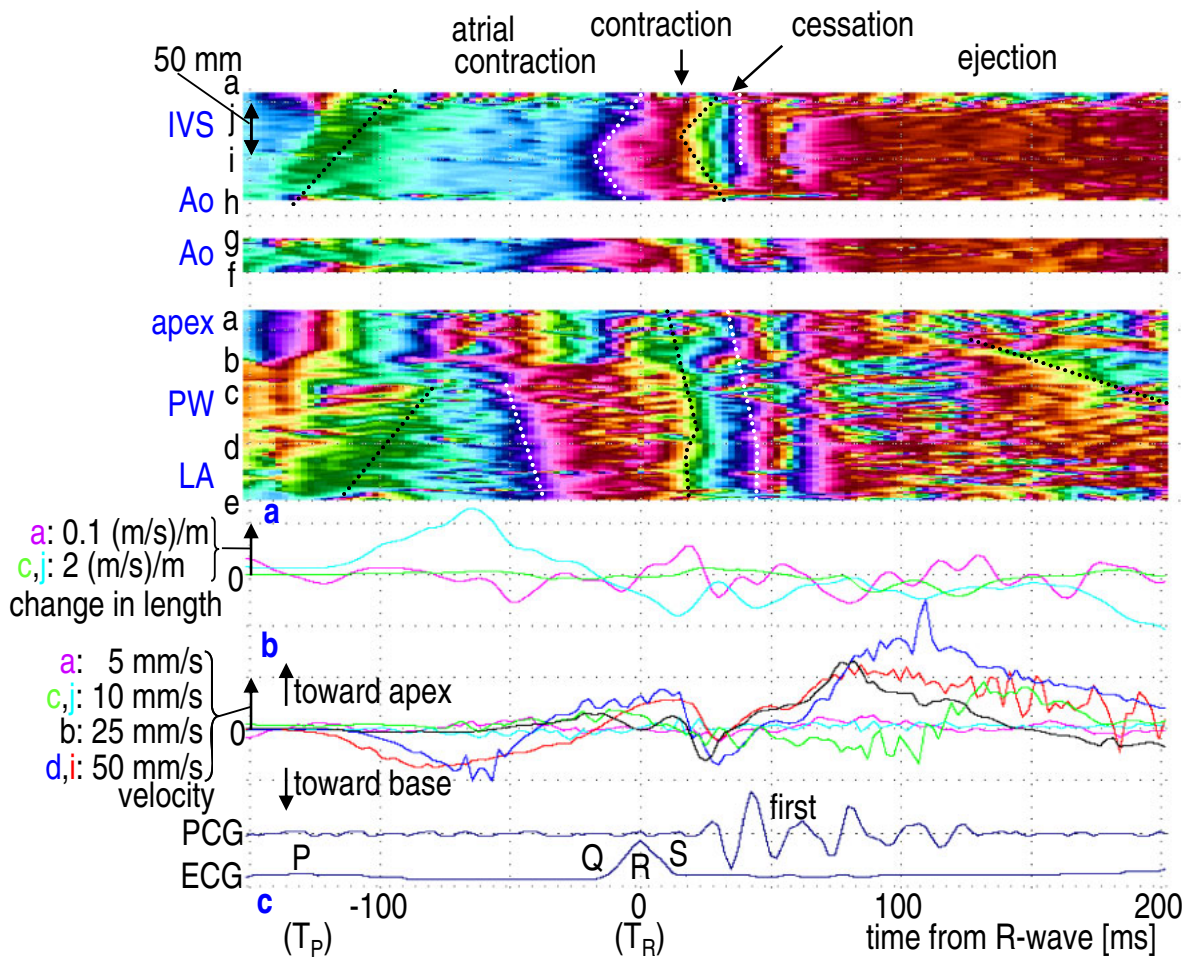


Fig. 2. (Color online) Expanded version of Fig. 1 at the beginning of the contraction. (a) Temporal changes in the phase of the 40-Hz component of the velocity wave in Fig. 1(b). (b) Temporal changes in thickness or length at points a–j in Fig. 1(d). (c) Velocity waveform at points a–j.

electrocardiography, there is downward velocity component (toward the base), corresponding to the LV expansion due to atrial contraction. After this, during systole, the upward velocity component (toward the apex) begins, which corresponds to the LV contraction, continuing until the time of the second heart sound, T_{II} , the time of the aortic valve closure, which is followed by rapid filling and slow filling phases, where these points moves downward (toward the base).

However, there are some differences among these transient times from downward to upward or from upward to downward at the base-side points (d or i). To clearly show these time differences regardless of the minuteness of the velocity, by applying the moving short-time Fourier transform to each of the velocity waveforms, simultaneously measured at all points set along the lines (a–b–c–d–e, g–f, and a–j–i–h) in Fig. 1(a), the phase of the 40-Hz component is color-coded, and its temporal change is shown in Fig. 1(b). Red shows the upward velocity component toward the probe (point O) in Fig. 1(a), and light blue shows its reverse property. As shown in Fig. 1(b), the onset time of the upward velocity (contraction) before time of R-wave of the electrocardiography, T_R , does not coincide at all points (a–j), but there are some propagating components in the LV.

By expanding the time axis in Figs. 1(b) and 1(d), the transition properties around T_R are shown in Figs. 2(a) and 2(c), respectively. At the same time, the instantaneous

change in length (shortening due to contraction or extension) is obtained at the points (a, c, j) shown in Fig. 2(b). The white dotted lines in Fig. 2(a) show the onset of the contraction determined by confirming whether the red component of velocity is associated with the change in length from extension to contraction as in Fig. 2(b). The black dotted lines show the reverse phenomenon.

From T_P , the atrial contraction begins and the LV volume increases, corresponding to the downward velocity (light green) in Fig. 2(a) to show the extension both in the posterior wall (b–c–d) and the interventricular septum (IVS) (a–j–i). Then, from the time 80 ms prior to T_R , the upward velocity component is generated at the apical side (a), and then from the time of 50 ms prior to T_R , the upward component propagates from the apex (b) to the base (e) along the LV posterior wall with a speed of about 9 m/s, where it is accompanied by the transition from extension to contraction. It then propagates along the IVS from point (i) to both the apex (a) and the base (h) at a speed of about 3 m/s. Just after passage of this component, the contraction begins at each point. The starting point (a) of the velocity component accompanying the contraction in Fig. 2(a) would be close to the terminal of the Purkinje fibers (special electrical conducting cells which rapidly transmit an electrical excitation).²⁶⁾ These velocity and change in length are too minute to be identified by other methods.

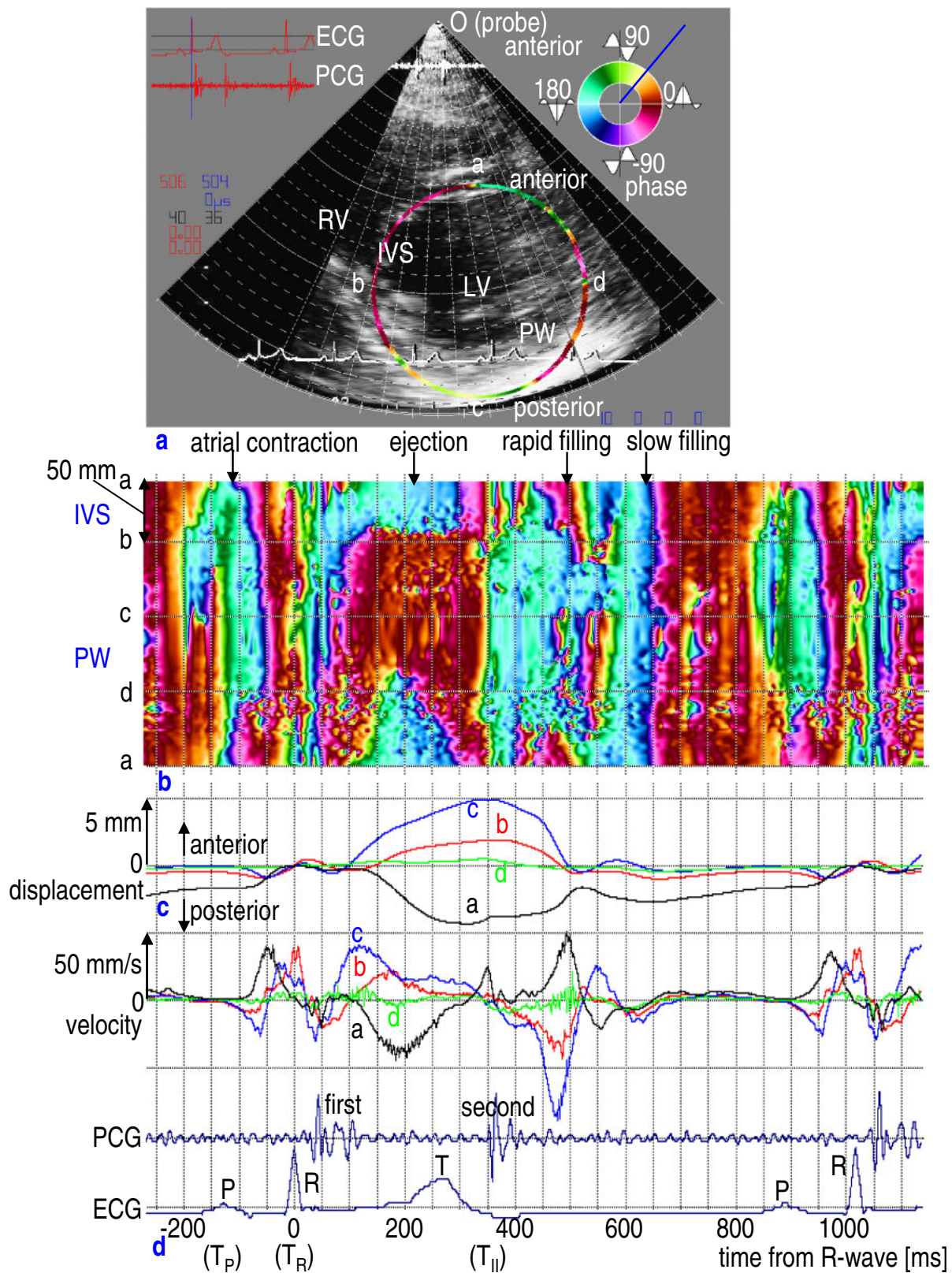


Fig. 3. (Color online) Time sequence of velocity and displacement in the unfolded left ventricular wall made based on the short-axis view. (a) Short-axis cross-sectional plane on the LV with the papillary muscle level. (b) For one cardiac cycle, the temporal changes in the phase of the velocity component. Vertical axis corresponds to the colored line in (a). (c) Displacement waveform at points a–d in (a). (d) Velocity waveform at points a–d.

The first heart sound following the QRS-complex is traditionally thought to be primarily associated with mechanical vibrations resulting from the closure of the mitral valve and the opening of the aortic valve.²⁷⁾ As shown in Fig. 2(a), after T_R , two waves are generated and propagate

from the apex (a) to the base (e) along the LV posterior wall. During the short period of 20 ms from the beginning of the first heart sound, the contraction property, which begins at the above onset in Fig. 2(a), is reversed. This “cessation of the contraction” would correspond to the LV expansion

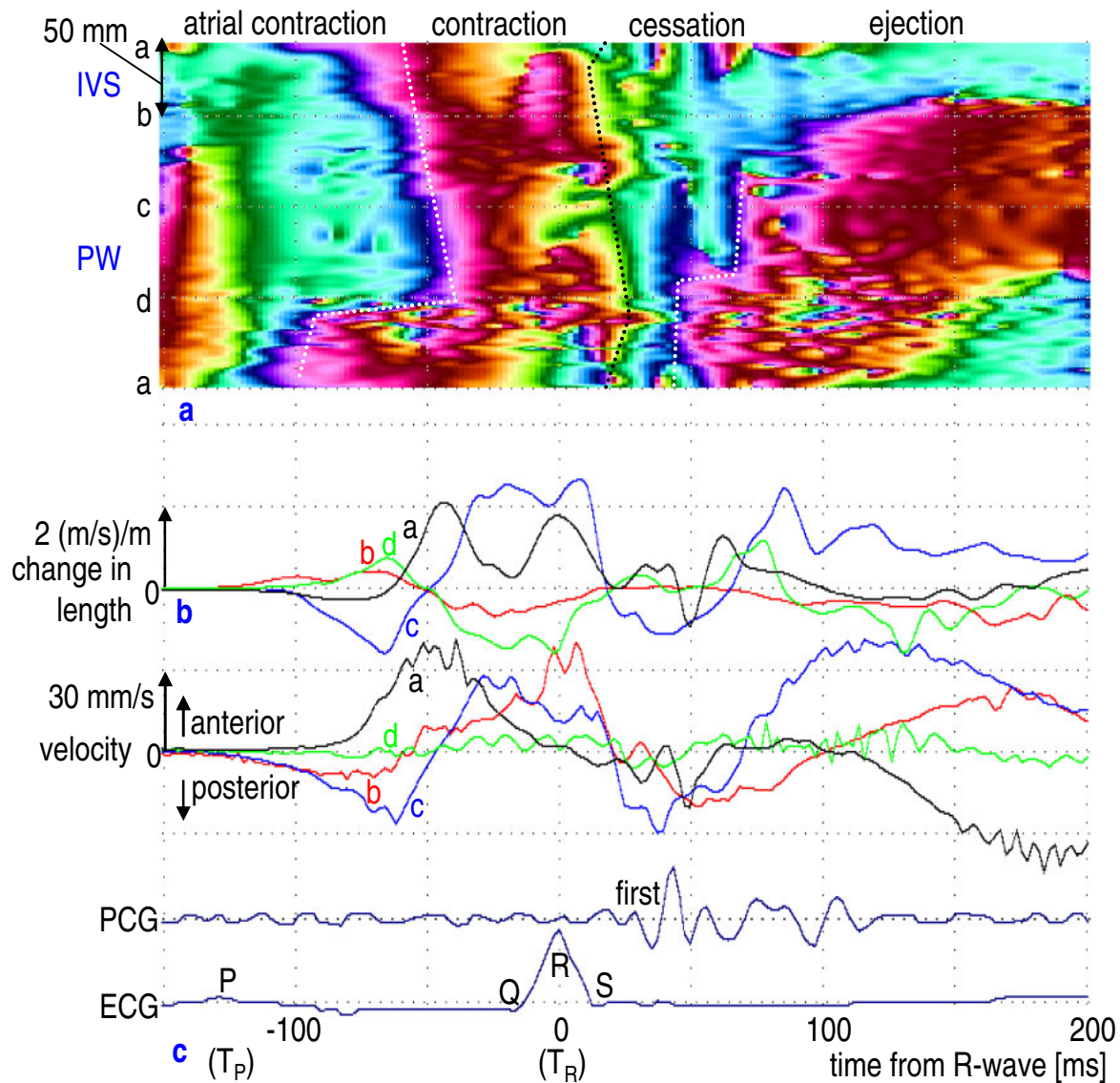


Fig. 4. (Color online) Expanded version of Fig. 3 at the beginning of the contraction. (a) Temporal changes in the phase of the velocity component in Fig. 3(b). (b) Typical waveforms of the change in thickness at point c and change in length at point b. (c) Velocity waveform measured at points a–d.

in the pre-ejection period that is necessary to cause the mitral valve closure.²⁸⁾ This cessation is terminated by the beginning of the second component of the above two waves, and after this cessation, all the points have the upward velocity components [red in Fig. 2(a)], that is, the contraction restarts, which constitutes the substantial LV contraction in the ejection period.

For the same subject, the position and the direction of the ultrasonic probe are changed so that the velocity and change in thickness are measured in the parasternal short-axis cross-sectional plane of the LV, as shown in Fig. 3(a). Figures 3(d) and 3(b) respectively show the velocity waveforms at four points (a–b–c–d) in Fig. 3(a) and temporal changes in the phase of the velocity waveform for one cardiac cycle. Figure 3(c) shows the displacement waveforms at these points. Roughly, during the ejection period, the LV contraction is associated with the downward displacement (to posterior) at point (a) and upward displacement (to anterior) at points (b, c), while point (d) is almost motionless.

By expanding the time axis in Fig. 3, the mechanical excitation is shown in Fig. 4 around T_R . From a time 120 ms

prior to T_R , the response propagates from the IVS (a), to the posterior wall (b–c–d) with a speed of about 6 m/s in the counterclockwise direction when viewed from the apical side. The propagation is *unidirectional*, that is, the contraction propagates in one direction (counterclockwise), not in both directions. The passage of the component [blue in Fig. 4(a)] is accompanied by thickening (at a and c) or contraction (at b and d) along the ultrasonic beam; both correspond to the contraction.

4. Discussion

Previous studies have defined the pre-ejection period^{28,29)} as the interval from the onset of the QRS-complex to the time of the aortic valve opening. It has been shown that myocardial acceleration during isovolumic contraction (IVA), which onset coincides with the initial upstroke of the LV pressure and the R-wave of the ECG, is clinically useful to measure LV contractile function that is unaffected by preload and afterload changes.^{30,31)} The importance of the present study is not to measure the pre-contraction or the IVA but to measure the spatial and temporal distribution of

the onsets of the IVA to show its excitation propagation. The end of the cessation in Figs. 2(a) and 4(a) corresponds to the traditionally accepted onset time of the contraction.^{12,13)} However, the minute contraction propagation occurring prior to the onset time was found in the present study. Physiologically, it is well known that the depolarized action potentials, cyclically generated at the sino-atrial node, propagate to the Purkinje fibers, which form interweaving networks on the endocardial surface of both ventricles and transmit the impulse to the ventricular endocardium. Their conduction velocity is 2.0–4.0 m/s in the normal human.^{32,33)} Around the time of the Q-wave, based on cell-to-cell connections, the action potential starts to propagate with a lower speed of 0.3–1.0 m/s in humans³³⁾ to the entire wall from the Purkinje fiber-myocyte junctions on the IVS surface, where the Purkinje fibers are in contact with the myocardium. In the present study, however, the measured propagation velocity regarding the minute contraction is about 9 m/s, which is much faster than those electrical conduction velocities in the previous studies. These differences suggest that the measured propagation components prior to T_R would be “pre-contraction” prior to the full contraction of the ejection period. Since the physiological basis of the observed contraction sequence remains unclear, further mechanistic details will be necessary to better substantiate these findings.

In the present study, the heart walls were manually identified before applying the measurement method. For applying the analysis in the present study to a lot of subjects and animals, it is essential to develop a reliable method for the automated identification of the heart wall.^{34–37)}

In the present study, the measurement of the velocity components was restricted to the direction of the ultrasonic beam. Alternatively, the measurement has been expanded into the two-dimensional (2D) space recently.^{38–41)} It is, however, still difficult to measure the rapid and minute velocity components in the heart wall by these methods. For thorough analysis of the propagation of the minute mechanical-excitation wave-front, the heart wall velocity distribution should be measured in the 2D space with high temporal and spatial resolutions.⁴²⁾

With the novel echocardiography in the present study, the minute-contraction sequences of the myocardium were confirmed noninvasively. These results show great potential for thorough understanding of the principles of the cardiac contraction mechanism, as well as for noninvasive assessment of myocardial tissue damage in early stage of cardiomyopathy and myocardial infarction since it is known that myocardial isotonic velocity for the contraction is decreased in failing hearts.⁴³⁾ The biological implications of these observations also remain unclear. In order to elucidate the role of these contractions in the ventricular remodeling, similar experiments should be performed in infarcted hearts. Moreover, investigation of methods to modulate these contractions should be performed to determine any potential therapeutic value with biventricular pacing.

Acknowledgments

The authors wish to thank Dr. Hideyuki Hasegawa of Tohoku University for experimental contributions. The study was approved by the review committee of the

Graduate School of Engineering, Tohoku University and the healthy subjects gave informed consent. This study was partly supported by a Grant-in-Aid for Scientific Research from the Japan Society for the Promotion of Science (2008–2010, No. 20360181).

- 1) C. Ramanathan, R. N. Ghanem, P. Jia, K. Ryu, and Y. Rudy: *Nat. Med.* **10** (2004) 422.
- 2) R. A. Stratbucker, C. M. Hyde, and S. E. Wixson: *IEEE Trans. Bio-Med. Electron.* **10** (1963) 145.
- 3) L. T. Mahoney, W. Smith, M. P. Noel, M. Florentine, D. J. Skorton, and S. M. Collins: *Invest. Radiol.* **22** (1987) 451.
- 4) L. Axel and L. Dougherty: *Radiology* **171** (1989) 841.
- 5) M. B. Buchalter, J. L. Weiss, W. J. Rogers, E. A. Zerhouni, M. L. Weisfeldt, R. Beyar, and E. P. Shapiro: *Circulation* **81** (1990) 1236.
- 6) A. Wagner, H. Mahrholdt, T. A. Holly, M. D. Elliott, M. Regenfus, M. Parker, F. J. Klocke, R. O. Bonow, R. J. Kim, and R. M. Judd: *Lancet* **361** (2003) 374.
- 7) Y. Notomi, R. M. Setser, T. Shiota, M. G. Martin-Miklovic, J. A. Weaver, Z. B. Popovic, H. Yamada, N. L. Greenberg, R. D. White, and J. D. Thomas: *Circulation* **111** (2005) 1141.
- 8) G. R. Sutherland, M. J. Stewart, K. W. Groundstroem, C. M. Moran, A. Fleming, F. J. Guell-Peris, R. A. Riemersma, L. N. Fenn, K. A. Fox, and W. N. McDicken: *J. Am. Soc. Echocardiogr.* **7** (1994) 441.
- 9) C. Pislaru, M. Belohlavek, R. Y. Bae, T. P. Abraham, J. F. Greenleaf, and J. B. Seward: *J. Am. Coll. Cardiol.* **37** (2001) 1141.
- 10) M. J. Garcia, J. D. Thomas, and A. L. Klein: *J. Am. Coll. Cardiol.* **32** (1998) 865.
- 11) C. G. Fonseca, H. C. Oxenham, B. R. Cowan, C. J. Occlshaw, and A. A. Young: *Am. J. Physiol. Heart Circ. Physiol.* **285** (2003) H621.
- 12) B. T. Wyman, W. C. Hunter, F. W. Prinzen, and E. R. McVeigh: *Am. J. Physiol. Heart Circ. Physiol.* **276** (1999) H881.
- 13) J. J. M. Zwanenburg, M. J. W. Götte, J. P. A. Kuijter, R. M. Heethaar, A. C. van Rossum, and J. T. Marcus: *Am. J. Physiol. Heart Circ. Physiol.* **286** (2004) 1872.
- 14) J. J. Bax, T. A. Abraham, S. S. Barold, O. A. Breithardt, J. W. H. Fung, S. Garrigue, J. Górcsan III, D. L. Hayes, D. A. Kass, J. Knuuti, C. Leclercq, C. Linde, D. B. Mark, M. J. Monaghan, P. Nihoyannopoulos, M. J. Schaliq, C. Stellbrink, and C.-M. Yu: *J. Am. Coll. Cardiol.* **46** (2005) 2168.
- 15) K. Miyatake, M. Yamagishi, N. Tanaka, M. Uematsu, N. Yamazaki, Y. Mine, A. Sano, and M. Hiram: *J. Am. Coll. Cardiol.* **25** (1995) 717.
- 16) H. Kanai, S. Katsumata, H. Honda, and Y. Koiwa: *Acoust. Sci. Technol.* **24** (2003) 17.
- 17) H. Kanai, M. Sato, N. Chubachi, and Y. Koiwa: *IEEE Trans. Ultrason. Ferroelectr. Freq. Control* **43** (1996) 791.
- 18) H. Kanai: *IEEE Trans. Ultrason. Ferroelectr. Freq. Control* **52** (2005) 1931.
- 19) H. Kanai: *Ultrasound Med. Biol.* **35** (2009) 936.
- 20) H. Kanai, H. Hasegawa, N. Chubachi, Y. Koiwa, and M. Tanaka: *IEEE Trans. Ultrason. Ferroelectr. Freq. Control* **44** (1997) 752.
- 21) H. Kanai, Y. Koiwa, Y. Saito, I. Susukida, and M. Tanaka: *Jpn. J. Appl. Phys.* **38** (1999) 3403.
- 22) H. Kanai and Y. Koiwa: *Ultrasound Med. Biol.* **27** (2001) 481.
- 23) H. Kanai, H. Hasegawa, and K. Imamura: *Jpn. J. Appl. Phys.* **45** (2006) 4718.
- 24) H. Kanai, K. Sugimura, Y. Koiwa, and Y. Tsukahara: *Electron. Lett.* **35** (1999) 949.
- 25) H. Yoshiara, H. Hasegawa, H. Kanai, and M. Tanaka: *Jpn. J. Appl. Phys.* **46** (2007) 4889.
- 26) F. H. Netter: *A Compilation of Paintings on the Normal and Pathologic Anatomy and Physiology, Embryology, and Diseases of the Heart* (Ciba Pharmaceutical, Summit, 1969).
- 27) A. A. Luisada and F. Portaluppi: *The Heart Sounds: New Facts and Their Clinical Implications* (Praeger Scientific, New York, 1982).
- 28) E. W. Remme, E. Lyseggen, T. Helle-Valle, A. Opdahl, E. Pettersen, T. Vartdal, A. Ragnarsson, M. Ljosland, H. Ihlen, T. Edvardsen, and O. A. Smiseth: *Circulation* **118** (2008) 373.
- 29) A. M. Weissler, W. S. Harris, and C. D. Schoenfeld: *Circulation* **37** (1968) 149.
- 30) M. Vogel, M. M. H. Cheung, J. Li, S. B. Kristiansen, M. R. Schmidt, P. A. White, K. Sorensen, and A. N. Redington: *Circulation* **107** (2003) 1647.
- 31) E. Lyseggen, S. I. Rabben, H. Skulstad, S. Urheim, C. Risoe, and O. A. Smiseth: *Circulation* **111** (2005) 1362.
- 32) D. Durrer, R. T. van Dam, G. E. Freud, M. J. Janse, F. L. Meuler, and R. C. Arzbacher: *Circulation* **41** (1970) 899.

- 33) A. M. Katz: *Physiology of the Heart* (Lippincott Williams & Wilkins, Philadelphia, PA, 2001) 3rd ed., p. 518.
- 34) T. Kinugawa, H. Hasegawa, and H. Kanai: *Jpn. J. Appl. Phys.* **47** (2008) 4155.
- 35) R. J. Watson, C. C. McLean, M. P. Moore, T. Spencer, D. M. Salter, T. Anderson, K. A. A. Fox, and W. N. McDicken: *Ultrasound Med. Biol.* **26** (2000) 73.
- 36) K. R. Waters, S. L. Bridal, C. Cohen-Bacrie, C. Levrier, P. Fornès, and P. Laugier: *Ultrasound Med. Biol.* **29** (2003) 1521.
- 37) C. S. Hall, E. D. Verdonk, S. A. Wickline, J. E. Perez, and J. G. Miller: *J. Acoust. Soc. Am.* **101** (1997) 563.
- 38) L. N. Bohs, B. J. Geiman, M. E. Anderson, S. C. Gebhart, and G. E. Trahey: *Ultrasonics* **38** (2000) 369.
- 39) S. Langeland, J. D'hooge, H. Torp, B. Bijnens, and P. Suetens: *Ultrasound Med. Biol.* **29** (2003) 1177.
- 40) S. Langeland, J. D'hooge, T. Claessens, P. Claus, P. Verdonck, P. Suetens, G. R. Sutherland, and B. Bijnens: *IEEE Trans. Ultrason. Ferroelectr. Freq. Control* **51** (2004) 1537.
- 41) N. Nitta and T. Shiina: *Jpn. J. Appl. Phys.* **43** (2004) 3249.
- 42) Y. Honjo, H. Hasegawa, and H. Kanai: *Jpn. J. Appl. Phys.* **49** (2010) 07HF14.
- 43) J. F. Spann, Jr., R. A. Buccino, E. H. Sonnenblick, and E. Braunwald: *Circ. Res.* **21** (1967) 341.